International Journal of Engineering Trends and Technology
ISSN: 2231 – 5381 /doi:10.14445/22315381/IJETT-V69I2P207
Volume 69 Issue 2, 42-52, February 2021

The Efficiency of the Rayleigh-Ritz Method Applied to In-Plane Vibrations of Circular Arches Elastically Restrained against Rotation at the Two Ends

Ahmed. Babahammou[#1], Rhali. Benamar[*2]

[#*] *University Mohammed V in Rabat, E.M.I. BP 765, Rabat, Morocco*

[1]*ahmedbabahammou@gmail.com*, [2]*rhali.benamar@gmail.com*

Abstract: *The natural frequencies and mode shapes of in-plane vibration of thin circular arches elastically restrained against rotation at their ends are determined using the Rayleigh-Ritz method; the trial functions obtained is taken as particular solutions of the sixth order differential equation of arch vibrations corresponding to an opening angle equal to* $1\,rad$*. The arch axis is assumed to be inextensible, and the dimensions of the cross-section are supposed constant and small in comparison with the radius. The first frequency parameters of arches with different opening angles and torsional spring stiffnesses are determined and shown to compare well with the available literature. The effect of the rotational stiffness on the frequency parameter and mode shapes are determined and illustrated in the joint plots. The accuracy and relative simplicity of the RRM applied in a systematic way to such complicated problems is established, making it ready to use in more complex situations, such as those of arches with one or more added masses, with non-uniform cross-section, with variable radius or with point supports*

Keywords - *In-plane linear vibration, circular arches, Rayleigh-Ritz method, elastically restrained, frequency parameters, mode shapes.*

I. INTRODUCTION

Arches are among the basic structural elements encountered in various real-world applications, such as aerospace structures, bridges, tunnels, and roof structures. Recently, deployable antennas have evolved in aerospace engineering using arches to support the reflector surface [1]. In-plane vibrations of circular arches elastically restrained against rotation at the two ends have not been studied enough in literature. Wasserman [2] has found the lowest natural frequencies of in-plane vibrations of arches with flexibly supported ends by an exact and an approximate formula. De Rosa [3], [4] studied the free vibration of an arch with a varying cross-section resting on flexible supports by a simple method in which the arch is replaced by a set of rigid bars connected together by means of elastic cells. Karami [5] investigated this type of arch with varying cross-sections by the accurate general differential quadrature method (GDQM). This paper investigates in-plane vibrations of inextensible thin circular arches having a constant cross-section and elastically restrained against rotation at their two ends using the Rayleigh-Ritz method (RRM). The new choice of trial functions used here constitutes an interesting novelty of this work because it allows treating easily many practical situations, such as those of arches with one or more added masses, with non-uniform cross-sections, or having a variable radius or one or more point supports. This is expected to give designers a useful tool for an innovative and flexible design. The trial functions are taken as particular analytical solutions of the sixth-degree differential motion equation of inextensible arches. Consequently, the results of deep arches are given for the first time by RRM in these papers. The rest of this paper is organized as follows: In Section (2), the procedure adopted for finding the particular solutions verifying the end conditions for an arch with an opening angle $\theta = 1$ rad is exposed. Section (3) is dedicated to the RRM general formulation. In Section (4), numerical results corresponding to different opening angles and to different values of the end support elastic stiffnesses given and compared with the bibliography. Finally, new numerical results are provided to be used as benchmarks for future quantitative comparisons.

II. TRIAL FUNCTIONS OF ARCHES SIMPLY SUPPORTED IN ADDITION TO ROTATIONAL SPRING AT IT BOTH ENDS

A. presentation of the problem

The thin circular arch studied shown in Fig. (1) is simply supported and elastically restrained against rotation at its both ends, it has a constant radius R, an opening angle θ, Young's modulus E, a mass per unit length of ring segment ρ, and the second moment of inertia with respect to the neutral line of the cross-sectional area I. The neural line is supposed inextensible. The stiffnesses of the left and right elastically restrained ends are K_i and K_r respectively. The effect of shear deformation is assumed to be neglected, and the constant cross-section is supposed to be small in comparison with the radius. In these conditions, the radial

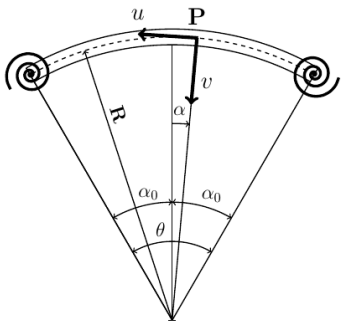

Fig. 1: The simply supported circular arch elastically restrained in rotation at its both ends

and tangential displacements u and v are related by [4], [6]:

$$u = \frac{\partial v}{\partial \alpha} \quad (1)$$

The purpose of this section is to determine the shape of the arch vibration solution.

B. Determination of the trial function for the RRM

The sixth order differential equation of the arch motion in terms of the in-plane displacement of a current point P defined by the curvilinear abscissa [4], [7]:

$$v^{(6)}(\alpha) + 2v^{(4)}(\alpha) + (1-\Omega^2)v^{(2)}(\alpha) + \Omega^2 v(\alpha) = 0 \quad (2)$$

where $v^{(n)}(\alpha)$ indicates the n^{th} the derivative of $v(\alpha)$, with respect to α, Ω is the non-dimensional frequency parameter such as $\Omega^2 = \frac{\rho R^4}{EI}\omega^2$And ω is the natural frequency. The sixth-degree characteristic polynomial associated with Eq (2) is:

$$X^3 + 2X^2 + (1-\Omega^2)X + \Omega^2 = 0 \quad (3)$$

The general solution of the differential Eq. (2) is [8]:

$$v(\alpha) = C_1\sinh(\lambda_1\alpha) + C_2\cosh(\lambda_1\alpha) + C_3\sin(\lambda_2\alpha) + C_4\cos(\lambda_2\alpha) + C_5\sin(\lambda_3\alpha) + C_6\cos(\lambda_3\alpha) \quad (4)$$

in which $p = \frac{1}{3} + \Omega^2$, $q = \frac{2}{27} - \frac{5}{3}\Omega^2$ and

$$\lambda_1 = \sqrt{Z_1 - \frac{2}{3}} \quad Z_1 = 2\sqrt{\frac{p}{3}}\cos\left(\frac{1}{3}\arccos\left(\sqrt{\frac{27q^2}{4p^3}}\right)\right)$$

$$\lambda_2 = \sqrt{-Z_2 + \frac{2}{3}} \quad Z_2 = 2\sqrt{\frac{p}{3}}\cos\left(\frac{2\pi}{3} - \frac{1}{3}\arccos\left(\sqrt{\frac{27q^2}{4p^3}}\right)\right)$$

$$\lambda_3 = \sqrt{-Z_3 + \frac{2}{3}} \quad Z_3 = 2\sqrt{\frac{p}{3}}\cos\left(\frac{2\pi}{3} + \frac{1}{3}\arccos\left(\sqrt{\frac{27q^2}{4p^3}}\right)\right)$$

The integration constants C_1 to C_6 are determined by the end conditions. The arch is supposed to be restrained against vertical and horizontal displacements and elastically restrained against rotations at both ends. This leads to [4], [9]:

at the end

$$\alpha = -\alpha_0 \quad v = v^{(1)} = 0, \quad M = -K_l\Psi \quad (5)$$

and at the end

$$\alpha = \alpha_0 \quad v = v^{(1)} = 0, \quad M = K_r\Psi \quad (6)$$

in which $M(\alpha)$ is the bending moment given by [4]:

$$M(\alpha) = -\frac{EI}{R^2}\left(v^{(3)}(\alpha) + v^{(1)}(\alpha)\right) \quad (7)$$

and $\Psi(\alpha)$ is the angle of rotation of the cross-section at the slope α due to the bending given by [4] :

$$\Psi(\alpha) = \frac{1}{R}(v^{(2)}(\alpha) + v(\alpha)) \quad (8)$$

Eqs. (5)-(8) can be summarized at the left end ($\alpha = -\alpha_0$) by [4]:

$$v = 0, \quad v^{(1)} = 0, \quad v^{(2)} - K_l^* v^{(3)} = 0 \quad (9)$$

and at right end ($\alpha = \alpha_0$) [5]:

$$v = 0, \quad v^{(1)} = 0, \quad v^{(2)} + K_r^* v^{(3)} = 0 \quad (10)$$

in which $K_l^* = \frac{K_l.R}{EI}$ and $K_r^* = \frac{K_r.R}{EI}$ are the dimensionless rotational stiffness at the left and right ends? The end condition calculations are very tedious because of the multiplicity of parameters involved, i.e., the seven unknowns C_1 to C_6, the frequency parameter Ω, and the arch geometrical and mechanical parameters such as the opening angle θ and the dimensionless rotational stiffnesses K_l^* and K_r^*. Symbolic calculations by a Matlab code made it possible to easily obtain a system of seven unknowns and six equations, written as :

$$[S].\{C\} = [0] \quad (11)$$

in which $\{C\}^T = (C_1, C_2; C_3, C_4, C_5, C_6)$ and $[S]$ is a 6×6 square Matrix. The solutions for Ω are deduced by stating the nullity of the matrix determinant. This leads to a transcendental equation solved numerically by the Matlab software to get the series of frequency parameters of the arch considered. Table (1) gives the first eight values of Ω_i found for arches with an opening angle $\theta = 1rad$ and different values of the dimensionless rotational stiffness $K_r^* = \frac{K_r.R}{EI}$ at right end and $K_l^* = \frac{K_l.R}{EI}$ at the left end. The corresponding normalized tangential and radial modes $v(\alpha^*)$, $u(\alpha^*)$, ($\alpha^* = \frac{\alpha}{\theta}$ varying from -0.5 to 0.5), are plotted in Fig. (2), for CS arch $K_l^* = \infty$ and $K_r^* = 0$ as an illustration of the series of basic functions used in the RRM applied below to various values of θ, K_l^* and K_r^*.

Table 1: Values of the first eight frequency parameters Ω_i obtained for circular arches with an opening angle $\theta = 1rad$ and various values of dimensionless rotational stiffness K^* Supposed equal at both ends.

K^*	Ω_1	Ω_2	Ω_3	Ω_4	Ω_5	Ω_6	Ω_7	Ω_7
0	42,415	85,394	160,88	243,51	358,31	480,45	634,67	796,31
6	50,839	92,528	171,11	252,35	369,16	490,11	645,84	806,49
12	54,794	96,708	177,62	258,54	377,10	497,53	654,64	814,80
24	58,595	101,38	185,30	266,53	387,72	508,04	667,40	827,12
∞	65,724	112,46	204,69	291,05	422,16	548,03	718,44	883,44

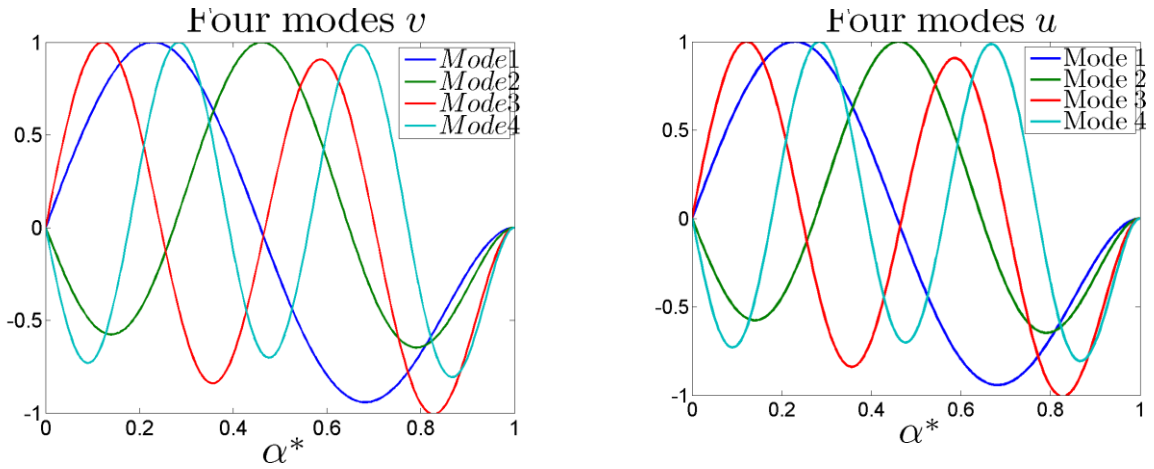

Fig. 2: First four tangential v and radial u displacements of CS arch with an opening angle $= 1rad$.

III. APPLICATION of the RRM to simply supported arches in addition to rotational restrains at both ends

The Rayleigh-Ritz method is a numerical method of finding approximations to eigenvalue equations that are difficult to solve analytically, particularly in the context of solving physical boundary value problems that can be expressed as matrix differential equations. It is used in mechanical engineering to approximate the eigenmodes of a physical system and the resonant frequencies of a structure.

3.1 General theory

Upon assuming harmonic motion, the tangential displacement $v(\alpha, t)$ of the current point of the arc axis $P(\alpha)$ can be expended in the form of a finite series:

$$v(\alpha, t) = a_i v_i(\alpha)\sin(\omega . t) \quad (12)$$

Repeated indexes are summed according to Einstein's convention, v_i is the i^{th} the trial function is given by :

$$v_i(\alpha) = C_1\sinh(\lambda_i\alpha) + C_2\cosh(\lambda_i\alpha) + C_3\sin(\gamma_i\alpha) + C_4\cos(\gamma_i\alpha) + C_5\sin(\kappa_i\alpha) + C_6\cos(\kappa_i\alpha) \quad (13)$$

corresponding to the frequency parameter Ω_i and a_i its contribution coefficient. The arch kinetic energy T is given by [10]:

$$T = \frac{1}{2}\rho\int_{-0.5l}^{0.5l}\left(\left(\frac{\partial v}{\partial t}\right)^2 + \left(\frac{\partial u}{\partial t}\right)^2\right)ds \quad (14)$$

The arch strain energy V which is the sum of the bending strain energy and the elastic energies stored in the torsional spring at the ends $\alpha = -\alpha_0$ and $\alpha = \alpha_0$. It is given by [10]:

$$V = \frac{1}{2}E.I\int_{-0.5l}^{0.5l}\left(\frac{\partial^2 u}{\partial s^2} + \frac{\partial}{\partial s}\frac{v}{R}\right)^2 ds + \frac{1}{2}K_l\left(\frac{\partial^2 v}{\partial \alpha^2}\right)^2_{\alpha=-\alpha_0} + \frac{1}{2}K_r\left(\frac{\partial^2 v}{\partial \alpha^2}\right)^2_{\alpha=\alpha_0} \quad (15)$$

in which $ds = Rd\alpha$ is the elementary length, $l = R\theta$ is total length and $u = \frac{\partial v}{\partial \alpha} = v^{(1)}$. Equations. (14)-(15) become:

$$T = \frac{\rho R}{2}\int_{-\alpha_0}^{\alpha_0}\left(\frac{\partial v}{\partial t}\right)^2 + \left(\frac{\partial v^{(1)}}{\partial t}\right)^2 d\alpha \quad (16)$$

$$V = \frac{E.I}{2R^3}\int_{-\alpha_0}^{\alpha_0}\left(v^{(3)} + v^{(1)}\right)^2 d\alpha + \frac{K_l}{2}\left(v^{(2)}\right)^2_{\alpha=-\alpha_0} + \frac{K_r}{2}\left(v^{(2)}\right)^2_{\alpha=\alpha_0} \quad (17)$$

Taking into account Eq.(12), the kinetic and the strain energies are discretized as follows:

$$T = \frac{1}{2}\omega^2 a_i a_j m_{ij}\cos^2(\omega t) \quad (18)$$

$$V = \frac{1}{2}a_i a_j k_{ij}\sin^2(\omega t) \quad (19)$$

m_{ij} , k_{ij}Are the mass and the linear rigidity tensors, respectively. There are given by :

$$m_{ij} = \rho R\int_{-\alpha_0}^{\alpha_0}\left(v_i v_j + v_i^{(1)}v_j^{(1)}\right)d\alpha \quad (20)$$

$$k_{ij} = \frac{E.I}{R^3}\int_{-\alpha_0}^{\alpha_0}\left(v_i^{(3)} + v_i^{(1)}\right)\left(v_j^{(3)} + v_j^{(1)}\right)d\alpha +$$

$$K_l\left(v_i^{(2)}v_j^{(2)}\right)_{\alpha=-\alpha_0} + K_r\left(v_i^{(2)}v_j^{(2)}\right)_{\alpha=\alpha_0} \quad (21)$$

The vibration problem is governed by Hamilton's principle [11]:

$$\delta\int_0^{\frac{2\pi}{\omega}}(V-T)dt = 0 \quad (22)$$

After the integration of the time functions over the range $\left[0,\frac{2\pi}{\omega}\right]$And the calculation of the derivatives with respect to the a_i's, one gets a linear eigenvalue problem, written in a matrix form as [11]:

$$2[K].\{A\} - 2\omega^2[M]\{A\} = \{0\} \quad (23)$$

$\{A\}^T = [a_1, a_2, \ldots, a_n]$ is the column vector of the basic function contribution coefficients. We must find [M] , [K] are the matrices associated with the tensors defined above. In order to facilitate the calculations, we define, as in Ref [11], the non-dimensional parameters α^* , m_{ij}^*, k_{ij}^* by:

$\alpha^* = \frac{\alpha}{\theta}$ the dimensionless angular abscissa.

$v_i^* = \frac{v_i}{R}$ the i^{th} dimensionless trial arch modes.

$m_{ij}^* = \frac{m_{ij}}{\rho R^3}$ The dimensionless general term of the mass tensor.

$k_{ij}^* = \frac{k_{ij}}{\rho R^3}$ The dimensionless general term of the rigidity tensor.

The frequency parameter Ω defined above is given by:

$$\Omega^2 = \frac{\rho R^4}{EI}\omega^2 \quad (24)$$

Has to be determined in what follows. The expressions for the dimensionless mass and rigidity tensors are:

$$m_{ij}^* = \theta\int_{-0.5}^{0.5} v_i^* v_j^* d\alpha^* + \frac{1}{\theta}\int_{-0.5}^{0.5} v_i^{*(1)} v_j^{*(1)} d\alpha^* \quad (25)$$

$$k_{ij}^* = \frac{1}{\theta}\int_{-0.5}^{0.5} v_i^{*(1)} v_j^{*(1)} d\alpha^* + \frac{1}{\theta^3}\int_{-0.5}^{0.5}\left(v_i^{*(1)} v_j^{*(3)} + v_j^{*(1)} v_i^{*(3)}\right) d\alpha^* + \frac{1}{\theta^5}\int_{-0.5}^{0.5} v_i^{*(3)} v_j^{*(3)} d\alpha^* + \frac{1}{\theta^4}\left(K_l^* v_i^{*(2)} v_j^{*(2)}\right)_{(\alpha^*=-0.5)} + \frac{1}{\theta^4}\left(K_r^* v_i^{*(2)} v_j^{*(2)}\right)_{(\alpha^*=0.5)} \quad (26)$$

The dimensionless form of Eq.(23) is expressed by:

$$[K^*]\{A\} - \Omega^2[M^*]\{A\} = \{0\} \quad (27)$$

Eq(27) represents the Rayleigh-Ritz formulation of the linear vibration problem. It is a linear algebraic system that has to be solved numerically to get the eigenvalues $\Omega_i = \omega_i\sqrt{\frac{\rho}{EI}}R^2$ and the eigenvectors {A}.

IV. NUMERICAL RESULTS AND DISCUSSION

A computer program has been written, based on the RRM presented above, to calculate the results of the linear arch vibration Eq numerically (27), corresponding to thin circular arches elastically restrained against rotation at their two ends. It is a linear Eigenvalue issue that has been solved numerically using the Matlab software, leading to the eigenvalues $\Omega_i = \sqrt{\frac{\rho}{EI}}R^2\omega_i$ $(i = 1..N)$ and their associated eigenvectors. To check the convergence of the solution, in particular for the fundamental and second frequency parameters Ω_1 and Ω_2 of a CC circular arch, the relative difference is defined by:

$$\Delta_i\% = \frac{\Omega_i - \Omega_{ref}}{\Omega_{ref}} \times 100 \quad i = 1,2 \quad (28)$$

in which Ω_{Ref}, taken as references, is the fundamental and second frequency parameters given by the exact method of de Rosa [7]. N is the number of the trial arch function. Fig. (3) gives the curves of the relative difference Δ_1 and Δ_2 versus N for a CC circular arch with the variable value of the opening angle $\theta = 20°, 80°, 160°, 180°$. One can notice the rapid convergence. If only one trial arch function is used (the Rayleigh method), the error does not exceed 0.12%. The quick convergence is one of the strong points of the trial arch function choice in this work.

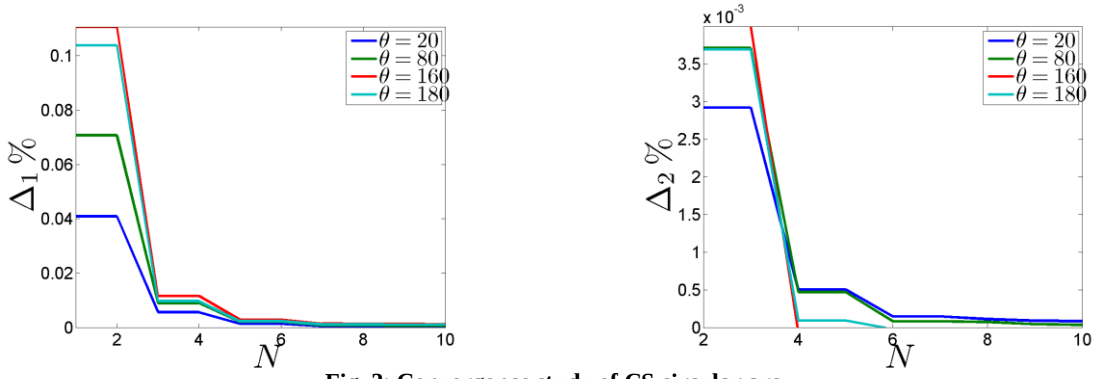

Fig. 3: Convergence study of CS circular arc

This convergence study can be investigated by the coefficient contributions a_i, when $N = 10$ trial arch functions are used to calculate the frequency parameters for an 180° Clamped-clamped arch. The contribution coefficient corresponding to different modes are listed in Table (2). The results show that the only significant contributions are those corresponding to the lowest modes. A second calculation made with $N = 3$ arch functions leads to the same coefficient contributions calculated before, which are summarized in Table (3).

Table 2: The contribution coefficient a_i for the CS circular arch with $\theta = 180^\circ$ with $N = 10$ trial arch functions

	Mode 1	Mode 2	Mode 3	Mode 4	Mode 5	Mode 6	Mode 7	Mode 8	Mode 9	Mode 10
a_1	1,0000	4,E-06	-4,E-01	-1,E-04	-3,E-01	-7,E-04	-3,E-01	-1,E-01	2,E-01	-2,E-01
a_2	-1,E-06	1,0000	-2,E-05	-9,E-02	-1,E-04	-8,E-02	-4,E-04	-6,E-02	-1,E-02	4,E-02
a_3	8,E-03	-2,E-07	0,9336	-1,E-04	-2,E-01	-4,E-04	-1,E-01	-6,E-02	8,E-02	-1,E-01
a_4	-2,E-07	2,E-03	-2,E-07	0,9956	-9,E-05	-5,E-02	-2,E-04	-3,E-02	-6,E-03	2,E-02
a_5	8,E-04	-9,E-09	2,E-02	2,E-05	0,9426	-4,E-04	-1,E-01	-4,E-02	5,E-02	-6,E-02
a_6	-2,E-07	1,E-04	-2,E-06	6,E-03	1,E-05	0,9952	-2,E-04	-2,E-02	-3,E-03	1,E-02
a_7	1,E-04	-5,E-06	3,E-03	-5,E-05	2,E-02	-3,E-04	0,9508	-5,E-02	4,E-02	-4,E-02
a_8	2,E-05	-7,E-06	3,E-04	8,E-04	2,E-03	5,E-03	7,E-03	0,7878	2,E-01	-1,E-03
a_9	1,E-05	-4,E-06	3,E-04	6,E-04	2,E-03	4,E-03	1,E-02	6,E-01	-0,9100	-7,E-02
a_{10}	1,E-06	4,E-07	2,E-05	4,E-05	1,E-04	2,E-04	1,E-03	4,E-02	-3,E-01	-0,9626

Table 3: The contribution coefficient a_i for the CS circular arch with $\theta = 180^\circ$ with $N = 3$ trial arch functions

	Mode 1	Mode 2	Mode 3
a_1	1,0000	7,E-11	4,E-01
a_2	3,E-12	-1,0000	9,E-11
a_3	8,E-03	-1,E-10	-0,9363

The fundamental frequency parameters Ω for a circular arch elastically restrained against rotation with opening angles $\theta = 40^\circ, 80^\circ, 120^\circ, 180^\circ$ are summarized in table (4), the dimensionless rotational stiffness is supposed to be identical at both ends $K_r^* = K_l^* = K^*$. The present results are compared with those obtained by several methods such as the generalized differential quadrature rule (GDQR) developed by Karami [5], the cell discretization method (CDM) applied by De Rosa [4], and the Galerkin method [4]. In general, the comparison is excellent. The percentage difference with the CDM, which gives lower bounds to the exact results, remains small; the present results are slightly less than those given by the Galerkin method. One can see that the advantage of the RRM applied here is that it leads to the frequency parameters with good precision for all opening angles. The first six mode shapes for SS, CC, and CS 90° This is illustrated in Fig (4). Table (5) lists the values of the fundamental frequency parameters Ω_1 for elastically restrained circular arches for a wide range of opening angles from $\theta = 20^\circ$ to 140°And for various values of the dimensionless rotational stiffness parameters supposed to be identical at both ends $K^* = K_l^* = K_r^*$. The results are compared with those given by De Rosa [3] and Wasserman [7]. In all cases, the percentage difference remains less than 3.22%; this value is noticed for a very big value of the rotational stiffness K^*. It is clear that the present results are very accurate because of their excellent comparison with the results given by the DQM [7] and those given by Ref[4].

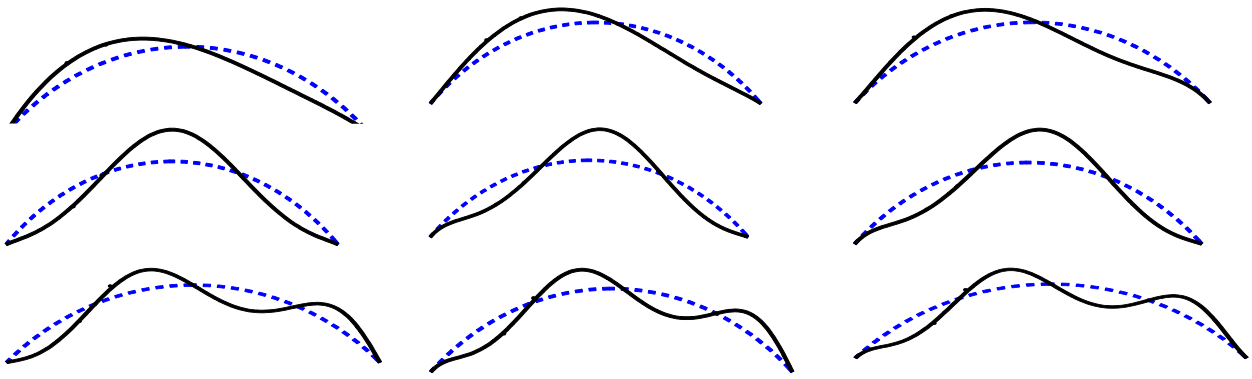

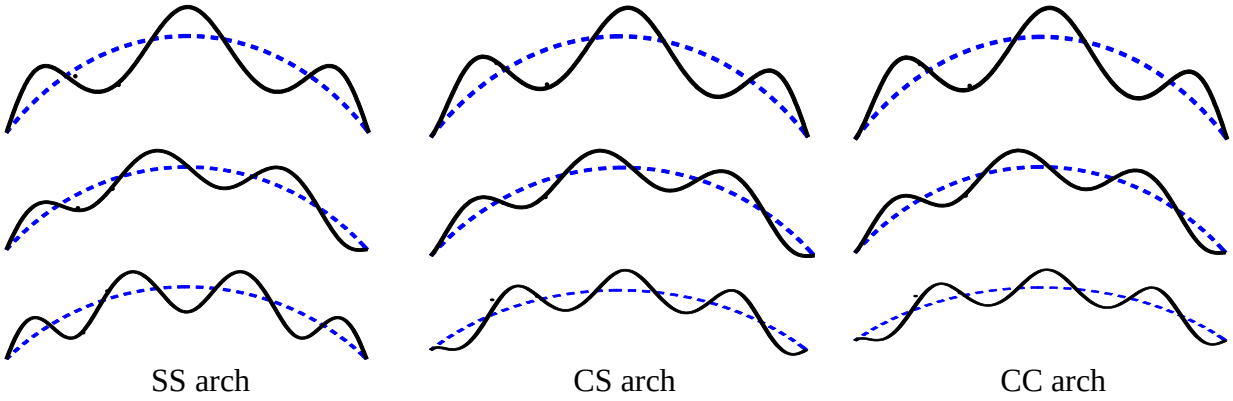

Fig. 4: The first fourth mode shapes of the 90° circular arches with variable rotational stiffness $K_r^* = K_l^* = K^*$.

Table 4: Fundamental frequency parameters $\Omega_1 = \omega_1\sqrt{\frac{\rho}{EI}}R^2$ for elastically restrained arches against rotation with identical dimensionless rotational stiffness at both ends $K_l^* = K_r^* = K^*$.

	$K^* = 0$				$K^* = 6$			
θ	Present	GDQR	CDM	Galerkin	Present	GDQR	CDM	Galerkin
40	78,5581	78,558	78,558	78,396	91,0774	90,954	90,692	91,972
80	17,9640	17,964	17,964	17,932	22,8178	22,788	22,713	23,345
120	6,9267	6,9268	6,9268	6,9168	9,6148	9,5407	9,5073	9,8534
	$K^* = 12$				$K^* = 24$			
θ	Present	GDQR	CDM	Galerkin	Present	GDQR	CDM	Galerkin
40	98,2578	98,014	97,676	100,17	106,2148	105,79	105,36	108,83
80	24,7671	24,711	24,612	25,489	26,4761	26,399	26,275	27,283
120	10,4635	10,337	10,293	10,719	11,1130	10,954	10,9	11,356
	$K^* = 100$				$K^* = \infty$			
θ	Present	GDQR	CDM	Galerkin	Present	GDQR	CDM	Galerkin
40	118,0861	117,71	117,09	121,23	123,9769	123,98	123,24	127,26
80	28,4494	28,383	28,225	29,268	29,2177	29,218	29,045	30,061
120	11,7382	11,599	11,534	11,778	11,8476	11,848	11,778	12,225

Fig. (5) displays the first four frequency parameters Ω_i, i = 1 to 4, as a function of the dimensionless rotational stiffness K^* Supposed to be identical at both ends, and this for several values of the opening angle θ. It may be noticed that the

The frequency parameter decreased when the arch was opening angle increases, but the rate of decrease is higher for small opening angles and very small for large opening angles. Also, the fundamental frequency increases with the torsional stiffness K^* but this growth is very small for large values of K^*. The first four mode shapes of 90° circular arches are plotted in Fig. (6) with an identical rotational stiffness K^* At both ends, taking the values $0,6,12,\infty$. The marine blue curve corresponds to SS circular arches, and the red curve corresponds to CC circular arches. One can conclude that the rotational stiffness affects the mode shapes slightly; in particular, the slop at the ends changes.

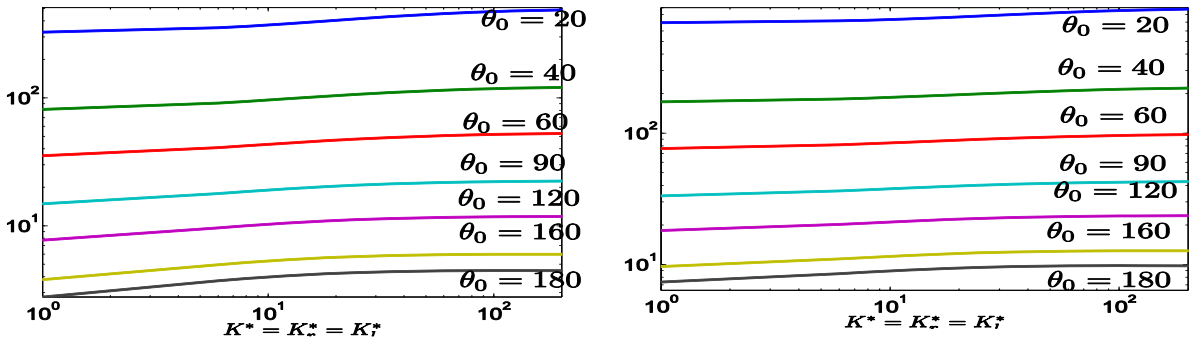

Fundamental frequency parameter Ω_1 **second frequency parameter Ω_2**

Fig. 5: The frequency curve as a function of the torsional stiffness assumed the same at the two ends for several values of opening angle θ.

Table 5: Fundamental frequency parameters $\Omega_1 = \omega_1\sqrt{\frac{\rho}{EI}}R^2$ for elastically restrained arches against rotation with identical dimensionless rotational stiffness at both ends $K_l^* = K_r^* = K^*$.

K^*		20	40	60	80	100	120	140
0	Present	321,521	78,560	33,627	17,965	10,777	6,927	4,654
	Ref [12]	321,520	78,556	33,615	17,967	10,780	6,928	4,655
	Ref [3]	320,827	78,396	33,560	17,932	10,759	6,917	4,647
6	Present	355,776	91,222	40,869	22,842	14,353	9,691	6,867
	Ref [12]	352,197	92,118	41,652	23,345	14,653	9,853	6,939
	Ref [3]	349,428	90,692	40,741	22,713	14,192	9,507	6,674
12	Present	382,947	98,523	44,268	24,808	15,630	10,580	7,517
	Ref [12]	375,762	100,170	45,491	25,489	15,969	10,719	7,534
	Ref [3]	370,109	97,677	44,099	24,612	15,374	10,293	7,221
18	Present	402,846	103,224	46,248	25,866	16,272	11,004	7,812
	Ref [12]	393,860	105,304	47,659	26,604	16,615	11,122	7,802
	Ref [3]	385,797	102,191	46,051	25,635	15,976	10,675	7,477
24	Present	417,560	106,487	47,545	26,522	16,653	11,244	7,973
	Ref [12]	408,028	108,826	49,044	27,283	16,997	11,356	7,954
	Ref [3]	398,116	105,357	47,329	26,275	16,340	10,900	7,625
∞	Present	503,578	123,984	53,744	29,220	17,928	11,849	8,232
	Ref [12]	516,561	127,260	55,218	30,061	18,470	12,225	8,505
	Ref [3]	500,560	123,240	53,423	29,045	17,821	11,778	8,184

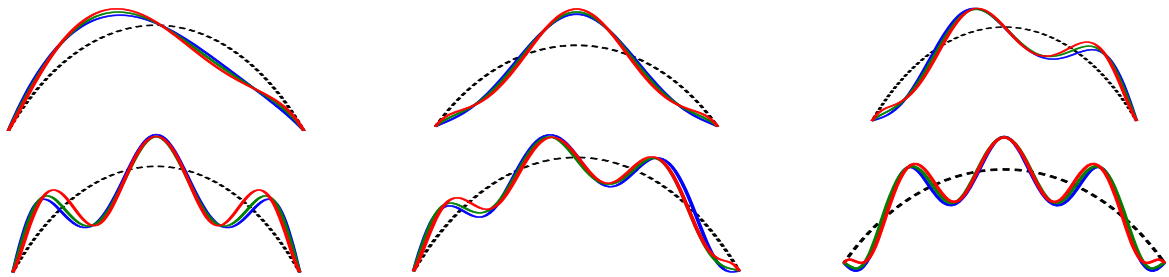

Fig. 6. The first six mode shapes of the 90° circular arches with variable rotational stiffness $K_r^* = K_l^* = K^*$. Dashed line: arch before deformation, blue line: arch with $K^* = 0$, green line: arch with $K^* = 12$, red line: arch with $K^* = \infty$,

The aim of this study was not only to present new trial arch functions used in the RRM. The purpose was also to provide new numerical results to be used as benchmarks for future quantitative comparisons. Table (6) gives the first five frequency parameters of elastically restrained arches with left ends having several values of the rotational stiffness K_l^* and the right ends are only simply supported ($k_r^* = 0$) for several values of the opening angle θ. The results of the first lines correspond to SS arches, and the results of the last lines correspond to CS arches. Table (7) lists the same results for various values of the rotational stiffness at the left end k_l^* and for a rotational stiffness at the right end k_r^* Having a very big value.

Table 6: First five frequency parameters Ω_i for arches with various values of the left dimensionless rotational stiffness K_l^* and right rotational stiffness $K_r^* = 0$.

First frequency parameter Ω_1								
K_l^*	$\theta = 20°$	$\theta = 40°$	$\theta = 60°$	$\theta = 80°$	$\theta = 100°$	$\theta = 120°$	$\theta = 160°$	$\theta = 180°$
0	321,515	78,558	33,626	17,964	10,776	6,927	3,218	2,267
6	337,196	84,763	37,202	20,351	12,501	8,239	4,056	2,962
12	349,441	88,235	38,815	21,261	13,073	8,623	4,253	3,108
18	358,775	90,436	39,725	21,736	13,354	8,804	4,340	3,172
24	365,656	91,930	40,309	22,027	13,521	8,907	4,387	3,205
100	392,969	97,158	42,139	22,853	13,948	9,148	4,475	3,261
∞	405,756	99,582	42,940	23,178	14,091	9,210	4,478	3,254
Second frequency parameter Ω_2								
K_l^*	$\theta = 20°$	$\theta = 40°$	$\theta = 60°$	$\theta = 80°$	$\theta = 100°$	$\theta = 120°$	$\theta = 160°$	$\theta = 180°$
0	690,011	171,150	75,077	41,465	25,923	17,495	9,154	6,923
6	703,312	176,694	78,421	43,791	27,667	18,867	10,084	7,713
12	715,268	180,484	80,348	44,964	28,454	19,429	10,404	7,964
18	724,717	183,075	81,550	45,651	28,893	19,730	10,568	8,090
24	733,852	185,218	82,433	46,108	29,163	19,902	10,649	8,149
100	773,742	193,377	85,435	47,518	29,919	20,342	10,819	8,258
∞	796,969	197,896	86,969	48,158	30,209	20,474	10,833	8,251
Third frequency parameter Ω_3								
K_l^*	$\theta = 20°$	$\theta = 40°$	$\theta = 60°$	$\theta = 80°$	$\theta = 100°$	$\theta = 120°$	$\theta = 160°$	$\theta = 180°$
0	1293,512	321,540	141,584	78,640	49,545	33,773	18,160	13,976
6	1310,900	328,812	145,974	81,685	51,818	35,550	19,350	14,981
12	1327,230	334,130	148,737	83,399	52,984	36,393	19,841	15,370
18	1341,929	338,146	150,606	84,473	53,677	36,874	20,108	15,579
24	1353,763	341,186	151,951	85,212	54,133	37,177	20,262	15,695
100	1417,629	354,619	156,960	87,545	55,338	37,820	20,413	15,734
∞	1458,743	362,676	159,748	88,772	55,967	38,187	20,593	15,881
Fourth frequency parameter Ω_4								
K^*	$\theta = 20°$	$\theta = 40°$	$\theta = 60°$	$\theta = 80°$	$\theta = 100°$	$\theta = 120°$	$\theta = 160°$	$\theta = 180°$
0	1987,738	495,553	219,229	122,522	77,767	53,464	29,317	22,811
6	2003,429	502,266	223,384	125,480	80,034	55,280	30,587	23,904
12	2018,683	507,509	226,249	127,341	81,356	56,273	31,206	24,409
18	2029,482	511,012	228,085	128,494	82,152	56,855	31,553	24,688
24	2045,664	515,096	229,883	129,483	82,764	57,264	31,763	24,846
100	2120,142	531,386	236,150	132,478	84,342	58,115	31,937	24,848
∞	2177,741	543,017	240,296	134,352	85,324	58,700	32,249	25,122
Fifth frequency parameter Ω_5								
K_l^*	$\theta = 20°$	$\theta = 40°$	$\theta = 60°$	$\theta = 80°$	$\theta = 100°$	$\theta = 120°$	$\theta = 160°$	$\theta = 180°$
0	2913,521	726,539	321,578	179,878	114,325	78,745	43,425	33,918
6	2931,666	734,273	326,350	183,261	116,905	80,804	44,855	35,146
12	2949,839	740,541	329,794	185,512	118,512	82,016	45,617	35,771
18	2967,529	745,700	332,362	187,087	119,593	82,810	46,104	36,168
24	2982,091	749,863	334,369	188,269	120,365	83,349	46,401	36,399
100	3079,124	771,396	342,488	191,761	121,646	83,312	44,800	34,350
∞	3159,699	787,861	348,679	195,015	123,936	85,364	47,090	36,793

The results of the first lines correspond to SS arches, and the results of the last lines correspond to CC arches. Finally, Table (8) gives the same results for the variable value of the rotational stiffness supposed equal at both ends, the results of the first lines correspond to SS arches, and the results of the last lines correspond to CC arches.

Table 7: First five frequency parameters Ω_i for arches with various values of the left dimensionless rotational stiffness K_l^* and right rotational stiffness $K_r^* = \infty$.

First frequency parameter Ω_1								
K_l^*	$\theta = 20°$	$\theta = 40°$	$\theta = 60°$	$\theta = 80°$	$\theta = 100°$	$\theta = 120°$	$\theta = 160°$	$\theta = 180°$
0	405,756	99,582	42,940	23,178	14,091	9,210	4,478	3,254
6	422,978	106,407	46,892	25,826	16,010	10,672	5,413	4,027
12	436,723	110,360	48,752	26,888	16,684	11,129	5,650	4,205
18	446,630	112,807	49,801	27,452	17,028	11,357	5,766	4,292
24	455,715	114,705	50,500	27,771	17,189	11,440	5,785	4,298
100	480,795	119,970	52,473	28,720	17,718	11,766	5,938	4,411
∞	503,551	123,977	53,740	29,218	17,926	11,848	5,927	4,384
Second frequency parameter Ω_2								
K_l^*	$\theta = 20°$	$\theta = 40°$	$\theta = 60°$	$\theta = 80°$	$\theta = 100°$	$\theta = 120°$	$\theta = 160°$	$\theta = 180°$
0	796,981	197,899	86,970	48,159	30,210	20,475	10,833	8,251
6	809,954	203,316	90,260	50,464	31,951	21,854	11,778	9,057
12	821,925	207,145	92,233	51,682	32,780	22,451	12,125	9,331
18	831,975	209,908	93,525	52,429	33,263	22,788	12,314	9,479
24	840,715	212,052	94,432	52,902	33,538	22,957	12,382	9,522
100	879,948	220,677	97,755	54,517	34,434	23,501	12,622	9,694
∞	909,146	225,963	99,458	55,195	34,721	23,613	12,604	9,652
Third frequency parameter Ω_3								
K_l^*	$\theta = 20°$	$\theta = 40°$	$\theta = 60°$	$\theta = 80°$	$\theta = 100°$	$\theta = 120°$	$\theta = 160°$	$\theta = 180°$
0	1458,748	362,677	159,749	88,773	55,967	38,188	20,594	15,881
6	1477,052	370,280	164,334	91,954	58,343	40,046	21,836	16,929
12	1493,774	375,795	167,222	93,755	59,574	40,937	22,357	17,343
18	1505,114	379,200	168,895	94,746	60,222	41,386	22,597	17,526
24	1523,167	383,261	170,441	95,435	60,526	41,491	22,523	17,413
100	1496,720	378,618	167,838	93,102	58,173	39,099	20,265	15,318
∞	1637,277	407,117	179,364	99,708	62,893	42,943	23,207	17,923
Fourth frequency parameter Ω_4								
K_l^*	$\theta = 20°$	$\theta = 40°$	$\theta = 60°$	$\theta = 80°$	$\theta = 100°$	$\theta = 120°$	$\theta = 160°$	$\theta = 180°$
0	2177,831	543,038	240,306	134,358	85,328	58,703	32,251	25,124
6	2193,182	549,597	244,380	137,271	87,571	60,509	33,523	26,222
12	2208,554	554,851	247,262	139,157	88,921	61,529	34,167	26,750
18	2222,025	558,949	249,357	140,466	89,831	62,206	34,590	27,098
24	2235,295	562,517	250,966	141,332	90,326	62,483	34,628	27,065
100	2099,053	520,826	224,050	120,612	73,836	49,283	26,018	20,011
∞	2373,799	592,019	262,066	146,590	93,149	64,128	35,294	27,524
Fifth frequency parameter Ω_5								
K_l^*	$\theta = 20°$	$\theta = 40°$	$\theta = 60°$	$\theta = 80°$	$\theta = 100°$	$\theta = 120°$	$\theta = 160°$	$\theta = 180°$
0	3159,724	787,868	348,684	195,019	123,939	85,367	47,093	36,796
6	3178,747	795,855	353,584	198,480	126,570	87,459	48,532	38,026
12	3195,068	801,835	356,911	200,656	128,117	88,616	49,244	38,602
18	3194,317	802,240	357,094	200,559	127,760	88,011	48,143	37,260
24	3229,471	810,274	360,222	201,974	128,384	88,229	48,099	37,242
100	2329,716	581,084	257,981	144,892	92,444	63,883	35,399	27,693
∞	3419,198	852,493	377,236	210,958	134,051	92,324	50,933	39,803

V. CONCLUSIONS

This paper treats a semi-analytical solution for free in-plane vibrations of inextensible circular arches with a uniform cross-section. The ends of the arch are axially and vertically stationary and elastically restrained in rotation. The Rayleigh-Ritz method is applied using trial functions obtained from the solution of the sixth order differential equation governing the inextensible in-plane vibrations of the arch corresponding to an opening angle $= 1$ rad. Among the end conditions considered, the (SS), (CS), (CC) are examined, and a large interval of variation of the dimensionless rotational stiffness is investigated. The integration constants of the differential equation are determined in each case via an iterative numerical solution, based on the Newton-Raphson method of the transcendental frequency equation. The RRM used in this work with its test

functions has an advantage compared to the one developed by Laura since it gives excellent results even for deep arches. The frequency parameter increases strongly for small opening angles but decreases slightly for large opening angles. Also, it increases with the rigidity of the arch but from a value of the dimensionless rotational stiffness $K^* = 200$, it becomes insensitive to this stiffness, which allows us to conclude that moderate or energetic tightening at the arch clamped ends does not change its mode shapes and frequencies significantly. The rotational stiffness affects the mode shapes slightly.

Table 8: First five frequency parameters Ω_i for arches with various values of the dimensionless rotational stiffness $K_l^* = K_r^* = K^*$.

First frequency parameter Ω_1								
K^*	$\theta = 20^\circ$	$\theta = 40^\circ$	$\theta = 60^\circ$	$\theta = 80^\circ$	$\theta = 100^\circ$	$= 120^\circ\theta$	$\theta = 160^\circ$	$\theta = 180^\circ$
0	321,515	78,558	33,626	17,964	10,776	6,927	3,218	2,267
6	353,156	91,077	40,868	22,818	14,298	9,615	4,944	3,699
12	378,106	98,258	44,261	24,767	15,543	10,464	5,391	4,037
18	397,231	102,914	46,238	25,819	16,176	10,876	5,593	4,185
24	412,261	106,215	47,542	26,476	16,555	11,113	5,702	4,263
100	472,807	118,086	51,797	28,449	17,614	11,738	5,963	4,443
∞	503,551	123,977	53,740	29,218	17,926	11,848	5,927	4,384
second frequency parameter Ω_2								
K^*	$\theta = 20^\circ$	$\theta = 40^\circ$	$\theta = 60^\circ$	$\theta = 80^\circ$	$\theta = 100^\circ$	$= 120^\circ\theta$	$\theta = 160^\circ$	$\theta = 180^\circ$
0	690,011	171,150	75,077	41,465	25,923	17,495	9,154	6,923
6	715,844	182,042	81,669	46,057	29,372	20,214	11,003	8,495
12	739,506	189,542	85,483	48,383	30,936	21,329	11,638	8,993
18	757,805	194,725	87,937	49,807	31,857	21,969	11,991	9,267
24	774,148	198,733	89,665	50,745	32,437	22,359	12,198	9,427
100	855,839	215,678	96,048	53,844	34,175	23,430	12,688	9,781
∞	909,146	225,963	99,458	55,195	34,721	23,613	12,604	9,652
Third frequency parameter Ω_3								
K^*	$\theta = 20^\circ$	$\theta = 40^\circ$	$\theta = 60^\circ$	$\theta = 80^\circ$	$\theta = 100^\circ$	$= 120^\circ\theta$	$\theta = 160^\circ$	$\theta = 180^\circ$
0	1293,512	321,540	141,584	78,640	49,545	33,773	18,160	13,976
6	1328,503	336,115	150,380	84,745	54,106	37,343	20,552	15,997
12	1360,719	346,664	155,901	88,195	56,473	39,064	21,569	16,810
18	1389,165	354,655	159,694	90,405	57,911	40,069	22,130	17,248
24	1415,493	361,233	162,554	91,953	58,851	40,679	22,419	17,454
100	1546,840	389,334	173,335	97,235	61,821	42,506	23,242	18,040
∞	1637,277	407,117	179,364	99,708	62,893	42,943	23,207	17,923
Fourth frequency parameter Ω_4								
K^*	$\theta = 20^\circ$	$\theta = 40^\circ$	$\theta = 60^\circ$	$\theta = 80^\circ$	$\theta = 100^\circ$	$= 120^\circ\theta$	$\theta = 160^\circ$	$\theta = 180^\circ$
0	1987,738	495,553	219,229	122,522	77,767	53,464	29,317	22,811
6	2017,245	508,595	227,393	128,366	82,261	57,076	31,855	25,000
12	2048,572	519,212	233,129	132,053	84,851	58,995	33,012	25,926
18	2071,586	526,756	237,115	134,579	86,614	60,303	33,823	26,591
24	2095,529	533,293	240,181	136,366	87,787	61,135	34,311	26,986
100	2243,713	566,317	253,353	143,061	91,686	63,614	35,501	27,861
∞	2373,799	592,019	262,066	146,590	93,149	64,128	35,294	27,524
Fifth frequency parameter Ω_5								
K^*	$\theta = 20^\circ$	$\theta = 40^\circ$	$\theta = 60^\circ$	$\theta = 80^\circ$	$\theta = 100^\circ$	$= 120^\circ\theta$	$\theta = 160^\circ$	$\theta = 180^\circ$
0	2913,521	726,539	321,578	179,878	114,325	78,745	43,425	33,918
6	2950,038	742,019	331,111	186,626	119,462	82,834	46,244	36,328
12	2983,855	753,869	337,672	190,928	122,538	85,152	47,697	37,516
18	3016,025	763,715	342,725	194,094	124,742	86,793	48,730	38,374
24	3052,298	773,412	347,180	196,594	126,278	87,771	49,102	38,567
100	3246,333	817,520	364,936	205,600	131,434	90,929	50,357	39,315
∞	3419,198	852,493	377,236	210,958	134,051	92,324	50,933	39,803

REFERENCES

[1] Liu, Fushou and Jin, Dongping and Wen, Hao. Optimal vibration control of curved beams using distributed parameter models. Journal of Sound and Vibration, (2016) 384:15–27.

[2] De Rosa, MA. The influence of the support flexibilities on the vibration frequencies of arches. Journal of sound and vibration, 146(1)(1991) 162–169.

[3] Wasserman, Y. Spatial symmetrical vibrations and stability of circular arches with flexibly supported ends. Journal of Sound and Vibration, 59(2)(1978) 181–194.

[4] Auciello, NM and De Rosa, MA. Free vibrations of circular arches: a review. Journal of Sound and Vibration, 176(4)(1994) 433–458, 1994.

[5] Karami, G, and Malekzadeh, P. In-plane free vibration analysis of circular arches with varying cross-sections using differential quadrature method. Journal of Sound and Vibration, 274(2004) (3-5):777–799.

[6] Henrych, Josef. The dynamics of arches and frames, volume 2. Elsevier Science Ltd, (1981).

[7] De Rosa, MA and Franciosi, C. Exact and approximate dynamic analysis of circular arches using DQM. International Journal of Solids and Structures, 37(8)(2000) 1103–1117.

[8] Babahammou, Ahmed and Benamar, Rhali. Semi-Analytical Solution of In-Plane Vibrations of Circular Arches Carrying Added Point Masses. Procedia Manufacturing, (2020) 44:465–472.

[9] Laura, PAA and De Irassar, PL Verniere and Carnicer, R and Bertero, R. A note on vibrations of a circumferential arch with thickness varying in a discontinuous fashion. Journal of sound and vibration, 120(1)(1988) 95–105.

[10] Igor, AK. Olga, l. L., Formulas structural Dynamics., (2001).

[11] Benamar, R and Bennouna, M and White, RG. The effects of large vibration amplitudes on the mode shapes and natural frequencies of thin elastic structures, part II: fully clamped rectangular isotropic plates. Journal of sound and vibration, 164(2)(1993) 295–316.

[12] Wasserman, Y. Spatial symmetrical vibrations and stability of circular arches with flexibly supported ends. Journal of Sound and Vibration, 59(2)(1978) 181–194.